A Boundary-Constrained Swarm Robot with Granular Jamming

Mohammad Amin Karimi,[1] Vahid Alizadehyazdi,[2] Bruno-Pier Busque,[3]
Heinrich M. Jaeger,[2] and Matthew Spenko[1]

***Abstract*— This paper describes a new type of compliant and configurable soft robot, a boundary-constrained swarm. The robot consists of a sealed flexible membrane that constrains both a number of mobile robotic subunits and passive granular material. The robot can change the volume fraction of the sealed membrane by applying a vacuum, which gives the robot the ability to operate in two distinct states: compliant and jammed. The compliant state allows the robot to surround and conform to objects or pass through narrow corridors. Jamming allows the robot to form a desired shape; grasp, manipulate, and exert relatively high forces on external objects; and achieve relatively higher locomotion speeds. Locomotion is achieved with a combination of whegs (wheeled legs) and vibration motors that are located on the robotic subunits. The paper describes the mechanical design of the robot, the control methodology, and its object handling capability.**

I. Introduction

Soft robots are generally considered to be continuous, compliant, and configurable. To achieve these characteristics, most soft robots are comprised of elastomeric materials and compliant actuators. In contrast, this paper describes a new type of robot that exhibits those same characteristics, but achieves them via a *boundary constrained swarm*. In other words, the robot is a collective set of swarm robots whose overall shape is constrained by an elastic membrane. This design approach enables us to achieve full control over the motion and configuration of a highly conformable system with similar characteristics of a continuum elastic soft robot, while adding capabilities such as mobility, distributed sensing and control, and design scalability.

This is similar in concept to a paramecium, a single celled organism comprised of a pellicle (analogous to the elastic membrane) that encompasses various cell parts (analogous to robots on the interior of the elastic membrane) along with cilia on the outside of the pellicle that aid in locomotion (analogous to robots on the exterior of the membrane). The pellicle responds to and interacts with the environment, triggering overall shape changes and facilitating locomotion. The internal components are important for overall function, but their relative configuration is not. This allows for an effectively random, unstructured placement of the internal components, which in turn creates excellent morphability.

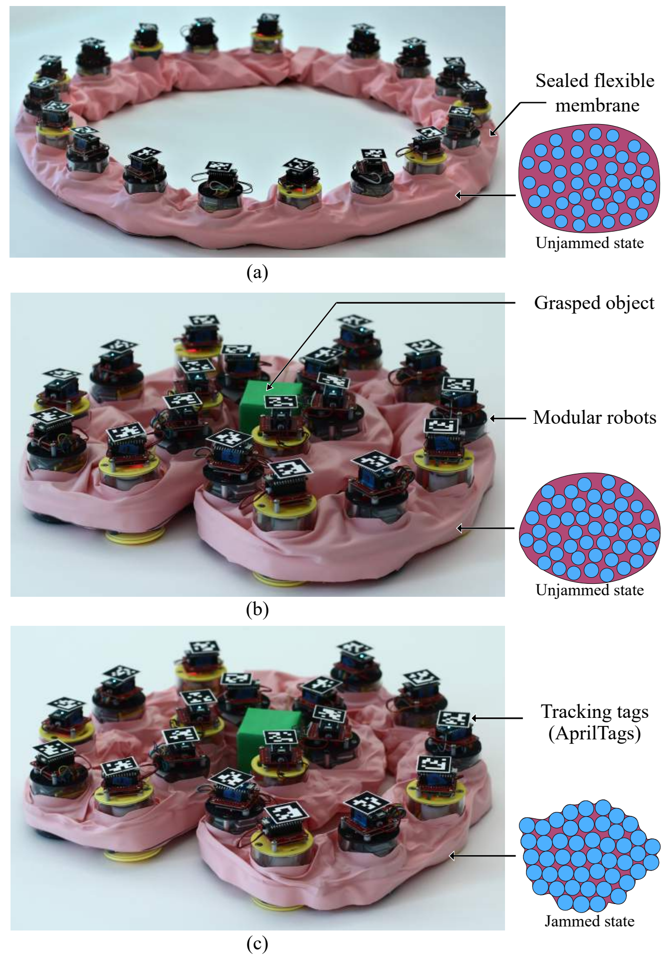

Fig. 1. The boundary-constrained swarm robot prototype. a) The robot in its default circular shape. b) The robot engulfing a cubic object in the unjammed state. In this state, there is less free space between passive particles compared with default circular shape. c) Vacuum granular jamming is on (20 mm passive particles are packed and their trace can be seen on membrane).

The prototype described here is comprised of 18 subunits embedded in a flexible membrane (see Fig. 1). Note that the design allows for larger numbers of subunits, which will better approximate a continuum robot. Collectively, the subunits determine the overall shape of the robot and enable locomotion through interaction with external surfaces. The result is a compliant, high degree-of-freedom system in which individual subunits can continuously reconfigure in response to external loads and each other's motion.

*This work is supported by NSF Grant No. 1830939.

[1]M. A. Karimi and M. Spenko are with the the Mechanical, Materials, and Aerospace Engineering Department, Illinois Institute of Technology, Chicago, IL 60616, USA. mkarimi1@hawk.iit.edu, mspenko@iit.edu

[2] V. Alizadehyazdi and H. M. Jaeger are with the James Franck Institute, The University of Chicago, Chicago, IL 60637, USA. vahid@uchicago.edu, h-jaeger@uchicago.edu

[3]B. P. Busque is with the Department of Mechanical Engineering, Université de Sherbrooke, QC J1K 2R1, Canada. Bruno-Pier.Busque@usherbrooke.ca

The constrained swarm embodies the continuum, compliant, and configurable properties found in soft robots, but in this state the robot is limited in its ability to manipulate objects due to the relatively low force it can apply to external objects. To address this, the robot also has the ability to execute a jamming phase transition, something few prior soft robots have demonstrated [1], [2], [3]. The robot exploits its ability to transition between soft (unjammed) and rigid (jammed) states to induce fluid-like flexibility or solid-like rigidity in response to objects in the environment.

Jamming occurs when a granular media's packing fraction exceeds a threshold that separates an unjammed state—characterized by particle arrangements that have a very low yield strength that allows for the particles to flow past each other—from a jammed state where the granular media exhibits solid-like behaviour with a finite yield strength [4], [5], [6]. This reversibly transforms a soft robotic system into a rigid structure with a yield strength far exceeding that of purely elastomeric systems. Importantly, jamming is controlled by the degree by which the passive particles are spatially confined by the membrane, and this in turn is controlled by a vacuum (other methods can also be employed) present in some of the subunit robots.

This paper describes the robot's mechanical design and control methodology as well as characterizes its ability to grasp and exert loads on objects. Section II highlights prior researches in modular robots and soft robots with jamming capability. Section III describes the robot's design and fabrication process. In Section IV, the control methodology is detailed. Experimental results that demonstrate the locomotion and object handling capabilities of the robot are covered in Section V, and Section VI concludes the work.

II. Related Work

This section covers previous work in jamming and self-reconfigurablity as they relate to soft robots.

A. Jamming in soft robots

There are two types of jamming-based variable stiffness systems: particle jamming and layer jamming [7]. Layer jamming mechanisms can increase the bending stiffness in one direction [8][9][10][11][12], while particle jamming is used where the physical properties are intended to be homogeneous. Particle jamming structures have been exploited in robotic manipulators due to their desirable stiffness variation, versatility, and design simplicity.

In one example of particle jamming, the "universal" gripper used a vacuum to initiate a volume change in a enclosed elastic membrane filled with ground coffee beans [13], [14]. The gripper was able to manipulate both smooth and complex-shaped objects in a variety of geometries. In a second example, a multi-segment controllable robotic arm was created that, similarly to the universal gripper, used an off-board vacuum pump as the jamming mechanism [15]. [16] designed a robotic arm using particle jamming by integrating the granular material into a McKibben actuator to both increase the load capacity and decrease the number of air lines needed. [17] proposed a passive mechanism to use particle jamming in a gripper arm for increasing the arm stiffness when gripping an object. The design works by attaching a soft, air pressure actuator to a pouch of granular material. [18] designed a portable (i.e. untethered) wearable joint with rubber granular material and variable stiffness control over the joint with jamming.

Similar to the prior work in granular jamming, our robot utilizes a built-in vacuum system to control the stiffness of its structure. However, the robot described here extends the concept of granular jamming by imagining what would happen if the particles, at least the ones on the boundary of the robot, had the ability to control their own movement.

B. Self-reconfigurable Robots

Self-reconfigurable robots are defined here as those that typically exhibit large degrees of freedom. An example is the flexible SMA-net robot proposed by [19], which used shape memory alloy springs to create a two-dimensional lattice shape. The shape memory alloy springs acted both as the soft skeleton and as the actuators of the robot. By creating a network of coupled oscillators, the robot was controlled through altering the phase differential of the actuators connected to the system. The control strategy was used to achieve an emergent behaviour similar to a slime mold amoeba. A modular robot with decentralized control was developed later by [20], which was able to move and switch between different locomotion modes through independent stiffness variation of its oscillatory subunits.

Some self reconfigurable robots deform themselves to be able to move, referred to as shape changing mobile robots. A group of researchers designed a spherical robot with multiple radial legs which enables the robot to move by continuously changing the length of its legs [21]. This robot demonstrated a novel type of locomotion with a continuous transition between contact points. Many research groups have also studied the development of soft-bodied, whole-skin robots [22], [23], [24], [25], which demonstrate locomotion by the deformation of their actual elastic membrane.

In this work, we use a decentralized modular design with an elastic membrane to achieve self-reconfigurability.

III. Design and Fabrication

A. Robot Design

The robot utilizes an active membrane formed by the subunit robots that controls enclosed passive particles. This controls the bulk motion of the passive granular material (hollow spheres) through locomotion of the robot as well as the mechanical properties of the granular media through particle jamming. This design can be cost efficient especially when scaling up the system, in that we can gain control over a large conformable system by only controlling the active units on its boundary and without controlling every individual passive particle. This can help when designing boundary constrained systems with large scale and fine discretization, which will even more closely resemble a continuum elastic soft robot while taking advantage of distributed sensing and control.

The robot uses two different subunit designs. Design A contains a vacuum pump to activate jamming and two vibration motors to facilitate locomotion (see Fig. 2). Design B has no vacuum and is only used for locomotion (see Fig. 3). The two subunit designs minimize the size of each subunit by distributing the hardware into separate compartments.

1) Jamming: The number of required vacuum subunits (Design A) was calculated based on the flow rate of each individual pump ($3.2\,\mathrm{L\,s^{-1}}$) and the total inner volume of the robot ($14.8\,\mathrm{L}^3$). Note that all the pump air inlets are connected to the robot in parallel, and therefore the number of pumps only affects flow rate. All other subunits were Design B. This resulted in eight design A subunits and ten design B subunits, which yielded a jamming time of less than 10 s to achieve vacuum gauge pressure of approximately $-20\,\mathrm{kPa}$. Prior experience and experimentation showed that this pressure results in acceptable jamming [14].

2) Locomotion: The vibration motors (present on both Design A and Design B) facilitate motion by reducing the friction of the modular units with ground. The whegs (Design B, see Fig. 3) act to move the subunit, and thus the larger robot. Whegs were used because they periodically come into contact with ground and can be completely enclosed inside the robotic sub-unit when not in use. Thus, robotic subunits that are not directly responsible for locomotion at a particular time step can simply stow the wheg inside the body of the robot and use their vibration motors to reduce the friction between the robot and surface. In contrast, wheels would permanently protrude from the bottom of the robotic subunit and render the vibration motors moot. To control the robot, we selectively activate each subunit's vibrator or wheg. The control methodology will be further detailed in Section IV.

3) Membrane Geometry: There are two main design factors in choosing the membrane geometry: the conformability of the robot and the maximum object grasping force. In order to achieve high conformability, the membrane is a torus as shown Fig. 1. Note that by increasing the outer diameter and decreasing inner diameter of the membrane, the robot's conformability decreases. Grasping force depends on many parameters including object size, object shape, robot inner diameter, robot outer diameter, membrane height, and membrane material. The effect of these parameters on grasping force will be studied in future work.

B. Fabrication Process

1) Subunit Design A: Design A is shown in Fig. 2. A WiFi-enabled microcontroller (Particle PHOTONH) enables wireless control of each subunit, and facilitates communication among subunits. The microcontroller is mounted on a battery shield (Sparkfun DEV-13626) which connects the battery to the micro-controller and enables charging. A 1000mAh lithium-ion battery coupled with a buck-boost converter (Sparkfun COM-15208) supplies a constant 5 V voltage to the system. Each subunit has two vibration motors (Parallex RB-Plx-314) which enable both speed and direction control over the subunit. A miniature vacuum pump (NW 9506) is used for jamming. The vibration motors and the vacuum pump are connected to a dual DC motor driver (Sparkfun TB6612FNG).

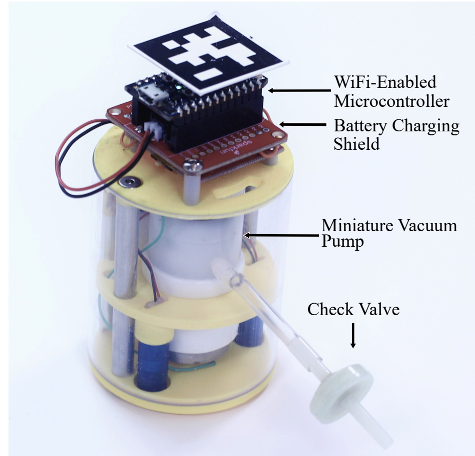

(a)

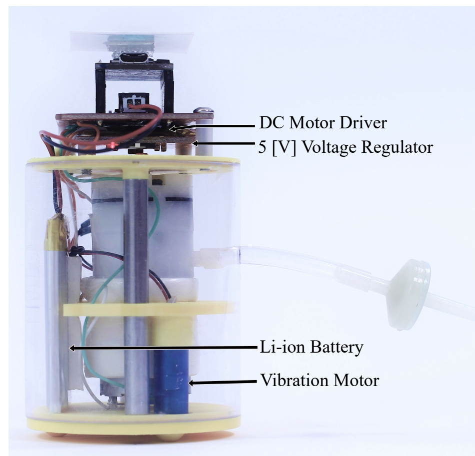

(b)

Fig. 2. Subunit Design A (a) perspective view (b) side view

2) Subunit Design B: Design B is shown in Fig. 3. A wheg is added to the design of this modular unit to increase the robot's driving force. To increase the traction force of the whegs, the mass of these sub-units is adjusted to 450 g by adding lead weights. Due to space limitations, the miniature vacuum pump is removed. A DC micro metal gearmotor (Polulu 2371) and an additional DC motor driver (Sparkfun ROB-14451) is used to control the speed and direction of the wheg. The rest of the hardware configuration is the same as Design A.

3) Membrane: The membrane was formed by heat sealing vinyl fabric into a torus shape with a major and minor radius of 30*cm* and 5*cm*, respectively. Mounting holes for the subunits were subsequently added on the membrane. The mounting holes are cut with a smaller diameter than the subunits in order to create an airtight seal after installation of the subunits. The subunits are passed through the mounting holes and the inner side of the membrane becomes com-

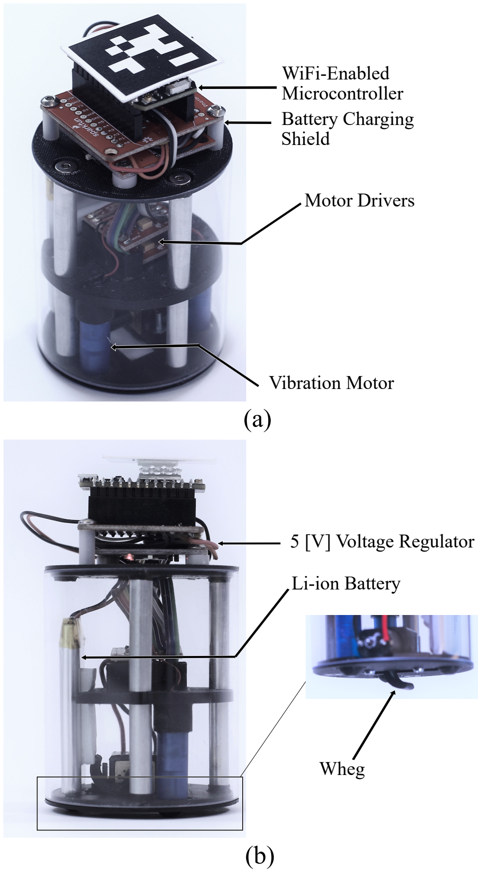

Fig. 3. Subunit Design B (a) perspective view (b) side view

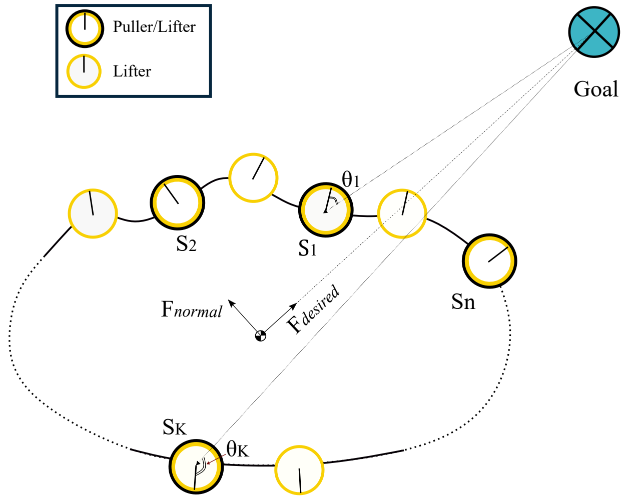

Fig. 4. The schematic of the system configuration and the position tracking parameters.

pletely sealed. 20 mm diameter hollow particles (CIC Ball PPH07870N) were added through one of the mounting holes before connecting the last subunit.

IV. Control

The controller was inspired by ants, who cooperatively work to carry food to their nest. While some ants only lift the object to facilitate the movement, others, the pullers, determine the direction of the group [26]. The lifters and pullers switch their roles periodically, depending on if they are able to provide thrust in the desired direction.

In each iteration of the control loop, the sub-robots are divided into those same two groups : *lifters* and *pullers* (see Fig. 4). At each time step, the relative heading angle of each robot is calculated with respect to the goal coordinate. The combination of sub-robots that results into the highest force in the desired direction $F_{desired}$, and the lowest force orthogonal to that direction, F_{normal}, are selected such that:

$$F_{normal}(\mathbf{c},\theta,\mathbf{f}) = \sum_{i=1}^{n}\left[c_i\left(f_i|\sin\theta_i|\right)\right]$$
$$F_{desired}(\mathbf{c},\theta,\mathbf{f}) = \sum_{i=1}^{n}\left[c_i\left(f_i|\cos\theta_i|\right)\right] \tag{1}$$

where n is the number of subunit robots with whegs, θ_i is the heading angle of subunit S_i, f_i is the total thrust of subunit S_i (if activating its wheg), c_i $(0 \leq c_i \leq 1)$ is the activation coefficient of subunit S_i, $\theta = [\theta_1, \theta_2, ..., \theta_n]^T$, $\mathbf{f} = [f_1, f_2, ..., f_n]^T$, and $\mathbf{c} = [c_1, c_2, ..., c_n]^T$.

This results in a linear constrained optimization problem, which is solved with the simplex optimization method. The optimization variables are the activation coefficients, c_i, which determine if subunit S_i provides thrust. The subunit will activate its wheg if the result is $c_i = 1$ (puller), or it will vibrate if $c_i = 0$ (lifter). To further simplify the problem, we assumed that the thrust of all the subunits are identical in both the forward and backward directions as well as normalized our objective function with respect to that thrust. The optimization problem can then be stated by Eq. (2).

$$\min_{\mathbf{c}}\left(\bar{F}_{normal}(\mathbf{c},\theta) - \bar{F}_{desired}(\mathbf{c},\theta)\right) \quad (0 \leq c_i \leq 1) \tag{2}$$

Note that the solution to a linear optimization problem is always on the vertices of the feasible region of the optimization variables. In other words, the solution to each activation coefficient c_i will always be either zero or one.

The optimization algorithm (see Algorithm (1)) only activates a few whegs to control the robot direction in each time step (similar to the puller ants). The subunits that were not selected to activate their whegs use their vibration motors instead to reduce their friction with ground, and therefore facilitate the movement for the rest of the system (similar to the lifter ants). If the vibration motors are not activated in this case, the number of selected subunits may not be able to overcome the overall friction of the inactive subunits.

Once one of the subunit robots approaches the object it stops moving. If at least one of the subunits has reached close enough to the target to stop, i.e. $\exists i : ||\mathbf{r_i} - \mathbf{r_d}|| < \varepsilon$, the system will start an "engulfing mode", in which the stopped subunit will become a center of rotation for the rest of the robotic subunits to engulf the target. This mode is performed by re-defining the target position as the position of the subunit that has stopped and calculating all the relative heading angles

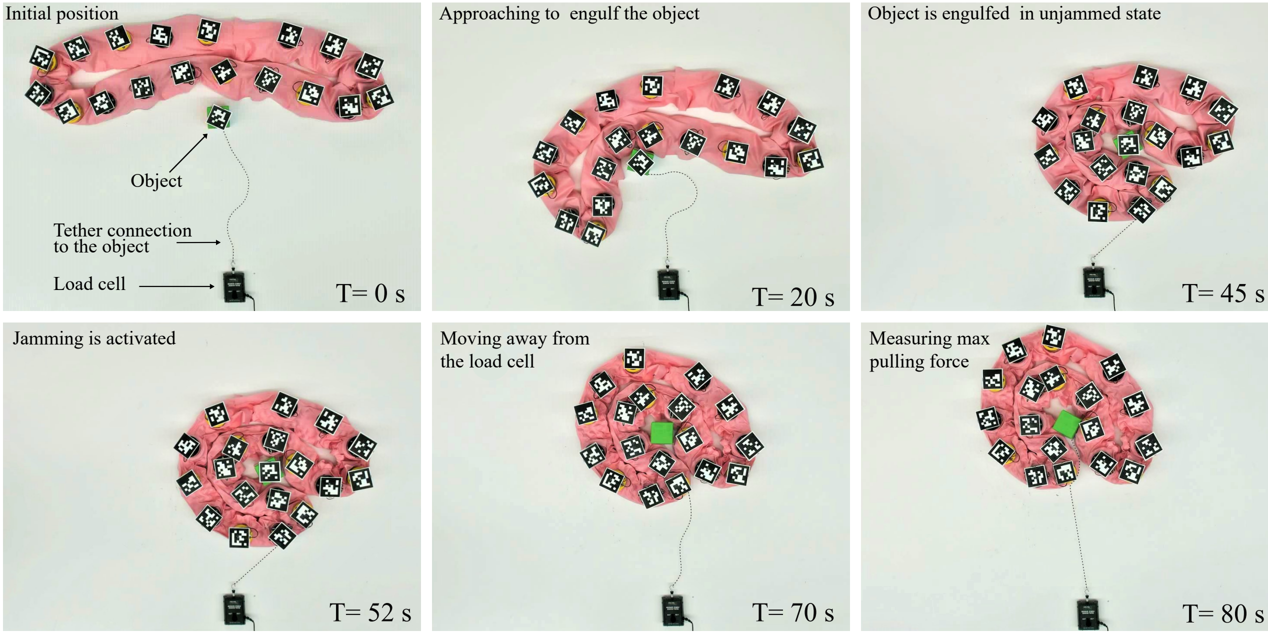

Fig. 5. Grasping and pulling an object. The robot starts from its initial configuration and approaches the object to engulf it (T=0-20s). After engulfing the object, the robot activates jamming to secure its grasping configuration (T=45-52s). The robot then moves away from the load cell and the maximum pulling force can be recorded once the tether connection is under tension. The tether connection between the object and the load cell is highlighted with a dashed line in this figure.

Algorithm 1 The position tracking algorithm

Given
- The position of the robotic subunits $\{\mathbf{r_1}, \mathbf{r_2}, \ldots, \mathbf{r_n}\}$
- The goal coordinate $\mathbf{r_d}$
- The relative heading angle the subunits with respect to the goal coordinate $\{\theta_1, \theta_2, ..., \theta_n\}$ $(-\pi \leq \theta_i \leq \pi)$
- Optimization variables $\{c_1, c_2, \ldots, c_n\}$ $(0 \leq c_i \leq 1)$

while $\bigcap_{i=1}^{n} ||\mathbf{r_i} - \mathbf{r_d}|| > \varepsilon$ **do**
  Compute the activation coefficients $\mathbf{c}$ from (2)
  for $i = 0$ to n **do**
    if $c_i = 1$ **then**
      Activate subunit S_i as puller
    else if $c_i = 0$
      Activate subunit S_i as lifter
    end if
  end for
  Stop all subunits
end while

($\theta_i' s$) with respect to that position. When multiple subunits have reached close enough to the initial target to stop, the updated target for the rest of the subunits is defined as the closest stopped subunit robot to each of them. The process will continue until all the subunits become closer than the defined threshold to the initial target.

V. Experimental Results

This section explains the testing procedures and the experiments conducted to characterize the robot's maneuverability, and object handling capabilities.

A. Testing platform

The robots moved on a flat surface covered with paper (Savage SAV461253). The robot's trajectory was tracked by a camera (Logitec Brio 960-001105) located above the testing platform. Real-time data processing for global localization, control, and communication with the subunits was performed within the ROS software platform. The force measurements in the object handling tasks were performed using a dual-range force sensor (Vernier SEN-12873).

B. Testing Procedures

Two tests were performed. The first measured the robot's position tracking capability. The second tested the robot's object handling abilities in both soft and rigid modes (unjammed and jammed states).

1) Position Tracking: Figure 5 shows how the robot approaches the object (T=0–20 s), engulfs it (T=45 s), performs a phase transition to jammed mode (T=52 s), then displaces and pulls the object (T=70–80 s). AprilTags were used to to measure the position and the direction of travel of the subunits (see Fig. 1, [27]). The system can track multiple tags simultaneously in real-time. The goal position was also specified by an AprilTag.

2) Object handling: The robot's jamming capability enables it to exert higher forces on objects and increase the robustness of object handling. To demonstrate this effect, the robot engulfs an object and pulls it away from a wall mounted sensor. The tests were performed to measure the maximum pulling force for a 58 x 58 x 82 mm cube in both jammed and unjammed states. The results of five trials each are shown in Fig. 6, which illustrates the effect of jamming

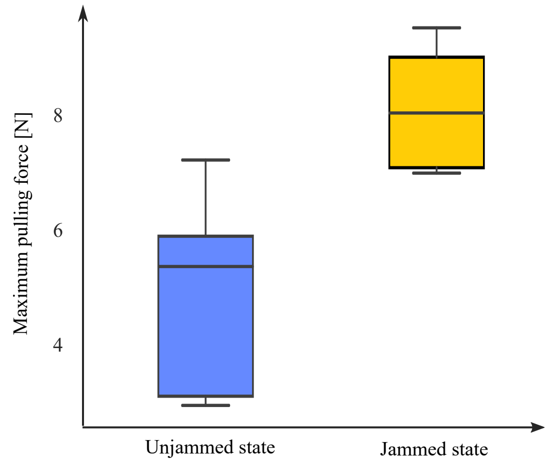

Fig. 6. The maximum pulling force of the robot compared in two jammed and unjammed states. The object used for the grasping was a 58 x 58 x 82 cm cube that was approached from its taller side (see Fig. 5)

on increasing the maximum pulling force, where we see a 50% increase with jamming activated.

VI. Conclusions

This paper presented a new type of soft robot where the general characteristics of a traditional elastomeric soft robot (compliant, configurable, and continuous) emerge from a set of boundary constrained modular sub-robots. A prototype illustrated how such a system can operate.

The robot design consists of eighteen modular units and passive granules constrained by an elastic membrane. A position tracking method inspired by ant colonies was implemented using linear optimization techniques to demonstrate the robot's ability to track an object from multiple directions. Experiments show the robot successfully engulfing and pulling an object from a wall mounted force sensor.

The capability to perform a phase transition from a soft to a rigid mode is also added to our design using granular vacuum jamming. The effect of jamming on the object handling force was studied, in which a 50% increase was observed in the maximum pulling force exerted on the aforementioned object.

Future studies will explore how the dynamic properties of the system can be tuned by the jamming phase transition. In addition, new prototypes will be developed to illustrate the boundary constrained swarm concept in three dimensions.

References

[1] S. Kim, C. Laschi, and B. Trimmer, "Soft robotics: a bioinspired evolution in robotics," *Trends in biotechnology*, vol. 31, no. 5, pp. 287–294, 2013.

[2] C. Majidi, "Soft robotics: a perspective—current trends and prospects for the future," *Soft Robotics*, vol. 1, no. 1, pp. 5–11, 2014.

[3] D. Rus and M. T. Tolley, "Design, fabrication and control of soft robots," *Nature*, vol. 521, no. 7553, p. 467, 2015.

[4] A. J. Liu and S. R. Nagel, "Nonlinear dynamics: Jamming is not just cool any more," *Nature*, vol. 396, no. 6706, p. 21, 1998.

[5] H. M. Jaeger, "Celebrating soft matter's 10th anniversary: Toward jamming by design," *Soft matter*, vol. 11, no. 1, pp. 12–27, 2015.

[6] M. Cui, T. Emrick, and T. P. Russell, "Stabilizing liquid drops in nonequilibrium shapes by the interfacial jamming of nanoparticles," *Science*, vol. 342, no. 6157, pp. 460–463, 2013.

[7] M. Manti, V. Cacucciolo, and M. Cianchetti, "Stiffening in soft robotics: A review of the state of the art," *IEEE Robotics & Automation Magazine*, vol. 23, no. 3, pp. 93–106, 2016.

[8] V. Wall, R. Deimel, and O. Brock, "Selective stiffening of soft actuators based on jamming," in *2015 IEEE ICRA*. IEEE, 2015, pp. 252–257.

[9] Y.-J. Kim, S. Cheng, S. Kim, and K. Iagnemma, "A novel layer jamming mechanism with tunable stiffness capability for minimally invasive surgery," *IEEE Transactions on Robotics*, vol. 29, no. 4, pp. 1031–1042, 2013.

[10] I. Choi, N. Corson, L. Peiros, E. W. Hawkes, S. Keller, and S. Follmer, "A soft, controllable, high force density linear brake utilizing layer jamming," *IEEE Robotics and Automation Letters*, vol. 3, no. 1, pp. 450–457, 2017.

[11] M. Bureau, T. Keller, J. Perry, R. Velik, and J. F. Veneman, "Variable stiffness structure for limb attachment," in *2011 IEEE ICORR*. IEEE, 2011, pp. 1–4.

[12] Y. S. Narang, J. J. Vlassak, and R. D. Howe, "Mechanically versatile soft machines through laminar jamming," *Advanced Functional Materials*, vol. 28, no. 17, p. 1707136, 2018.

[13] J. R. Amend, E. Brown, N. Rodenberg, H. M. Jaeger, and H. Lipson, "A positive pressure universal gripper based on the jamming of granular material," *IEEE Transactions on Robotics*, vol. 28, no. 2, pp. 341–350, 2012.

[14] E. Brown, N. Rodenberg, J. Amend, A. Mozeika, E. Steltz, M. R. Zakin, H. Lipson, and H. M. Jaeger, "Universal robotic gripper based on the jamming of granular material," *Proceedings of the National Academy of Sciences*, vol. 107, no. 44, pp. 18 809–18 814, 2010.

[15] N. G. Cheng, M. B. Lobovsky, S. J. Keating, A. M. Setapen, K. I. Gero, A. E. Hosoi, and K. D. Iagnemma, "Design and analysis of a robust, low-cost, highly articulated manipulator enabled by jamming of granular media," in *2012 IEEE ICRA*. IEEE, 2012, pp. 4328–4333.

[16] A. Jiang, G. Xynogalas, P. Dasgupta, K. Althoefer, and T. Nanayakkara, "Design of a variable stiffness flexible manipulator with composite granular jamming and membrane coupling," in *2012 IEEE/RSJ IROS*. IEEE, 2012, pp. 2922–2927.

[17] Y. Li, Y. Chen, Y. Yang, and Y. Wei, "Passive particle jamming and its stiffening of soft robotic grippers," *IEEE Transactions on Robotics*, vol. 33, no. 2, pp. 446–455, 2017.

[18] S. Hauser, M. Robertson, A. Ijspeert, and J. Paik, "Jammjoint: A variable stiffness device based on granular jamming for wearable joint support," *IEEE Robotics and Automation Letters*, vol. 2, no. 2, pp. 849–855, 2017.

[19] Y. Sato, T. Nagai, H. Yokoi, T. Mizuno, and Y. Kakazu, "A study on distributed sma-net robot control by coupled oscillator system," in *SICE 2000. International Session Papers (IEEE Cat. No. 00TH8545)*. IEEE, 2000, pp. 171–174.

[20] T. Umedachi, K. Ito, and A. Ishiguro, "Soft-bodied amoeba-inspired robot that switches between qualitatively different behaviors with decentralized stiffness control," *Adaptive behavior*, vol. 23, no. 2, pp. 97–108, 2015.

[21] H. Nozaki, Y. Kujirai, R. Niiyama, Y. Kawahara, T. Yonezawa, and J. Nakazawa, "Continuous shape changing locomotion of 32-legged spherical robot," in *2018 IEEE/RSJ IROS*. IEEE, 2018, pp. 2721–2726.

[22] D. S. Shah, M. C. Yuen, L. G. Tilton, E. J. Yang, and R. Kramer-Bottiglio, "Morphing robots using robotic skins that sculpt clay," *IEEE Robotics and Automation Letters*, vol. 4, no. 2, pp. 2204–2211, 2019.

[23] J. Hou, M. Luo, and T. Mei, "The design and control of amoeba-like robot," in *2010 International Conference on Computer Application and System Modeling (ICCASM 2010)*, vol. 1. IEEE, 2010, pp. V1–88.

[24] Y. Sugiyama, A. Shiotsu, M. Yamanaka, and S. Hirai, "Circular/spherical robots for crawling and jumping," in *2005 IEEE ICRA*. IEEE, 2005, pp. 3595–3600.

[25] E. Steltz, A. Mozeika, N. Rodenberg, E. Brown, and H. M. Jaeger, "Jsel: Jamming skin enabled locomotion," in *2009 IEEE/RSJ IROS*. IEEE, 2009, pp. 5672–5677.

[26] A. Gelblum, I. Pinkoviezky, E. Fonio, A. Ghosh, N. Gov, and O. Feinerman, "Ant groups optimally amplify the effect of transiently informed individuals," *Nature communications*, vol. 6, p. 7729, 2015.

[27] J. Wang and E. Olson, "Apriltag 2: Efficient and robust fiducial detection," in *2016 IEEE/RSJ IROS*. IEEE, 2016, pp. 4193–4198.